Electronic Supplementary Material (ESI) for RSC Advances.

Co Nanoparticles Decorated by N-dopted Carbon Nanotubes as High-Efficiency Catalyst with Intrinsic Oxidase-like Property for Colorimetric Sensing

Tao Chen, Jinmin Cao, Xiaofang Bao, Yu Peng, Li Liu* and Wensheng Fu*

Chongqing Key Laboratory of Green Synthesis and Applications, College of Chemistry, Chongqing Normal University, Chongqing 401331, China

Key words: Synergistic effect, Oxidase-like activity, Colorimetic sensing, Hybrid catalyst, Ascorbic acid detection.

Corresponding Authors

*E-mail: liliu1208@163.com (L. Liu.)

*E-mail: fuwensheng@cqnu.edu.cn (W. Fu.)

Experimental section

Chemicals and Materials

Zinc nitrate hexahydrate ($Zn(NO_3)_2·6H_2O$, AR), methanol (CH_3OH, AR), glacial acetic acid (CH_3COOH, AR), sodium acetate trihydrate ($CH_3COONa·3H_2O$, AR) were purchased from Chengdu Kelong Chemical Co., Ltd. 2-methyl imidazole ($C_4H_6N_2$, AR), cobalt nitrate hexahydrate ($Co(NO_3)_2·6H_2O$, AR) were purchased from Shanghai McLean Biochemical Technology Co., Ltd. 3,3',5,5' -tetramethylbenzidine dihydrochloride hydrate ($C_{16}H_{20}N_2·2HCl·xH_2O$, AR) was purchased from Shanghai Alding Biochemical Technology Co., Ltd., and concentrated hydrochloric acid (HCl, AR) was sourced from Chuandong Chemical. None of the reagents were further purified. Water used for the whole experiment (18.2m Ω·cm).

Characterization

X-ray diffractometer (XRD, LAB XRD-6100, Shimadu, Japan) and Raman spectroscopy were used to analyze the crystal phase of the product. Scanning electron microscopy (SEM, JSM-7800F, JEOL) and Transmission electron microscopy (TEM, Talos F200S, ThermoFisher Scientific) were used to characterize the morphology of the products. The morphology and composition of the products were obtained by energy-dispersive X-ray spectroscopy (EDX) coupling with high-angel annular dark-field scanning transmission electron microscopy (HAADF-STEM) (JEM-2100F, Japan). The valence states of the elements were analyzed by X-ray photoelectron spectroscopy (XPS, ESCALAB250Xi). The specific surface area and pore size distribution of the product were determined by N_2 adsorption-desorption isotherm (3H-2000PS1, Bestor Instrument Technology). The UV-visible spectrophotometer (UV-2550, Shimazu, Japan) was used to record the absorption spectra of catalytic oxidation reactions and to measure their catalytic performance.

Synthesis of solid ZIF-8 precursor

2.97 g (0.01 mol) $Zn(NO_3)_2·6H_2O$ and 3.075 g (0.0375 mol) $C_4H_6N_2$ were dissolved in 75 mL methanol, respectively. The two solutions were mixed and stirred at room temperature for 24 hours. Finally, the white powder obtained by centrifugation was washed with methanol for three times and dried in an oven at 60 ℃ for 12h to obtain ZIF-8 precursor with dodecahedron morphology.

Synthesis of core-shell ZIF-8@ZIF-67 intermediate

Firstly, 300 mg ZIF-8 precursor was dispersed evenly with 50 mL methanol and stirred for 10 min to obtain solution A. Then 0.363 g of $Co(NO_3)_2·6H_2O$ and 0.385 g of $C_4H_6N_2$ were dissolved in 50 mL methanol solution, respectively. Then the methanol solution of cobalt nitrate hexahydrate and the methanol solution of 2-methyl imidazole were slowly poured into the solution A, stirring for 24 hours at room temperature. The purple powder obtained by centrifugation was washed with methanol for three times and dried in an oven at 60℃ for 12h. Then, the ZIF-8@ZIF-67 core-shell dodecahedron was obtained.

Synthesis of hollow Co@N-CNTs hybrid dodecahedron framework

100 mg the core-shell ZIF-8@ZIF-67 core-shell intermediate was placed in tube furnace and heated to 700 °C with a heating rate of 5 °C min^{-1}, then the temperature was further increased up to 900℃ with a heating rate of 2℃/min and retained for 100 min under a N_2 flow. Finally, the hollow Co@N-CNTs hybrid dodecahedron framework was obtained.

Synthesis Co_3O_4@N-CNTs Contrast materials

100 mg the hollow Co@N-CNTs hybrid dodecahedron framework was heated to 250℃ with a heating rate of 5℃/min and retained for 60 min in air atmosphere. Then, the Co_3O_4@N-CNTs Contrast material was successfully synthesized.

Synthesis N-CNTs Contrast materials

100 mg Co_3O_4@N-CNTs was dissolved in 20 mL HCl solution and stirred at room temperature for 4h. The black powder obtained by centrifugation was washed with methanol for three times and then dried in an oven at 60℃ for 12h.

Study on oxidase-like activity of Co@N-CNTs catalyst

Using TMB as the substrate for color development, the oxidase-like activity of Co@N-CNTs hybrid catalyst was investigated. The absorbance was measured at 652 nm by UV-Vis spectrophotometer. Briefly, the 500 μL Co@N-CNTs (10 μg/mL), 500 μL 80 μg/mL TMB solution are added in the 500 μL HAc-NaAc buffer solution (pH=4) in turn. Then, the mixed solution was reacted at room temperature for 10min. Finally, the UV-Vis absorption peak at 652 nm was recorded.

Determination of stability and reusability of Co@N-CNTs catalyst

To evaluate the stability of the as-prepared catalyst, Co@N-CNTs (500 μL,10 μg/mL) suspension was mixed with TMB (500 μL, 80 μg/mL) in HAc-NaAc buffer solution (500 μL, pH = 4.0) and stored in an aqueous solution at room temperature. The UV-Vis absorption value at 652 nm was recorded every day to evaluate the stability of its catalytic performance. To further consider the reusability, Co@N-CNTs (500 μL,10 μg/mL) suspension was mixed with TMB (500 μL, 80 μg/mL) solution in HAc-NaAc buffer solution (500 μL, pH = 4.0) for 10 min to determine the UV-Vis absorption value at 652 nm. Then, after centrifugation, The Co@N-CNTs material was recovered by washing with ethanol, dried at 60℃ for 12h, and then the next cycle was determined according to the same method.

Detection of ascorbic acid (AA)

To detect ascorbic acid, the Co@N-CNTs catalyst (500 μL,10 μg/mL) was mixed with the TMB (500 μL, 80 μg/mL) solution and different concentrations of ascorbic acid (0.1~200 μM) in HAc-NaAc buffer solution (500μL, pH = 4.0). After reaction for 10 min at room temperature, the absorbance change of the system at 652 nm was measured and the catalytic reaction was monitored. The calibration curve of AA was obtained by plotting ΔA at 652 nm (ΔA = A_0−A,

where A_0 and A are the absorbance at 652 nm in the absence and presence of AA, respectively) as a function of the AA concentration.

Determination of AA in human serum by colorimetry

The determination of AA in human serum samples by colorimetry is as follows. Firstly, the treated human serum samples were diluted by a factor of 1000 with a buffer solution to keep the AA concentration was within the linear range of detection. The absorbance measurements were adopted.

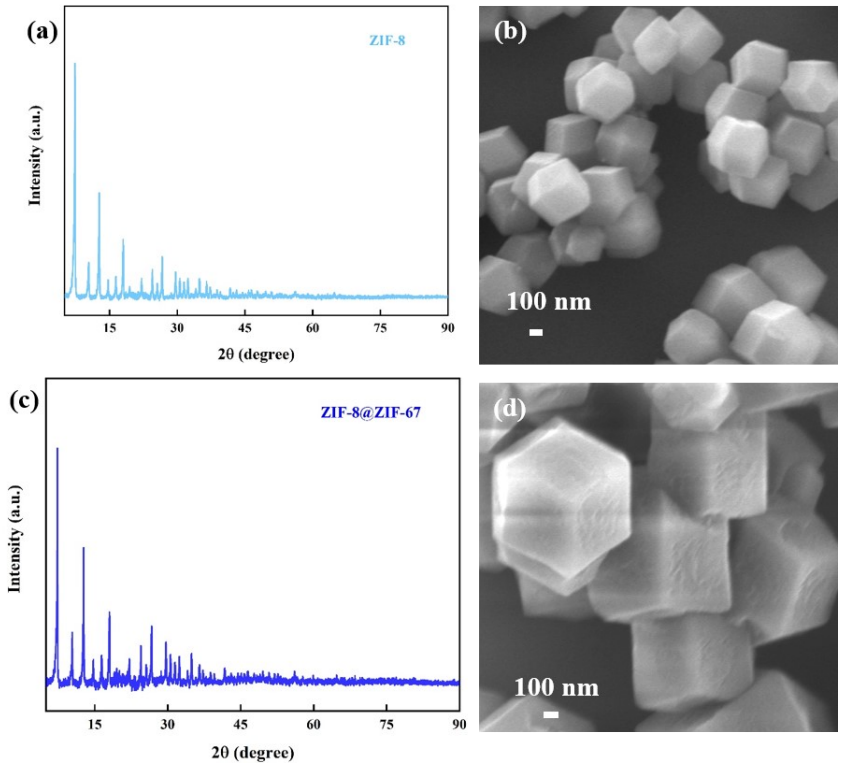

Figure S1. (a) The XRD pattern and (b) the SEM image of ZIF-8 dodecahedron precursor, (c) the XRD pattern and (d) the SEM image of ZIF-8@ZIF-67 core-shell dodecahedron.

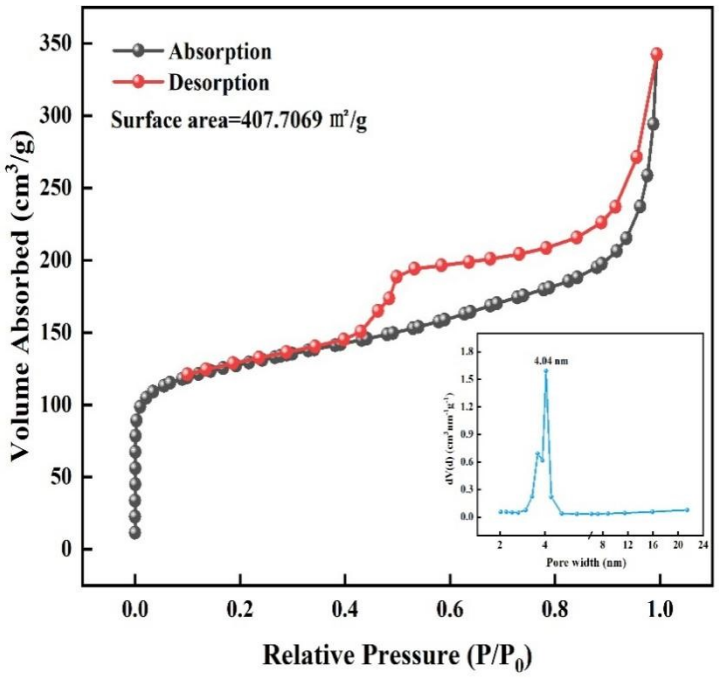

Figure S2. N_2 adsorption-desorption isotherm of the Co@N-CNTs hollow hybrid dodecahedron framework. The inset is the corresponding pore size distribution curve.

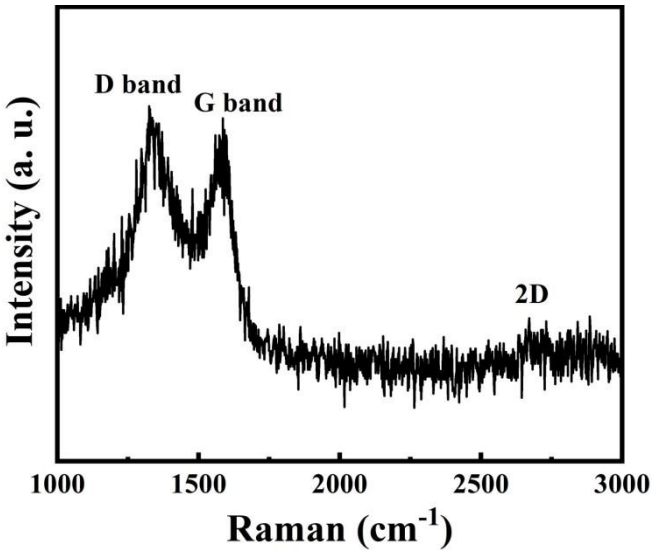

Figure S3. The Raman spectrum of the Co@N-CNTs hollow hybrid dodecahedron framework.

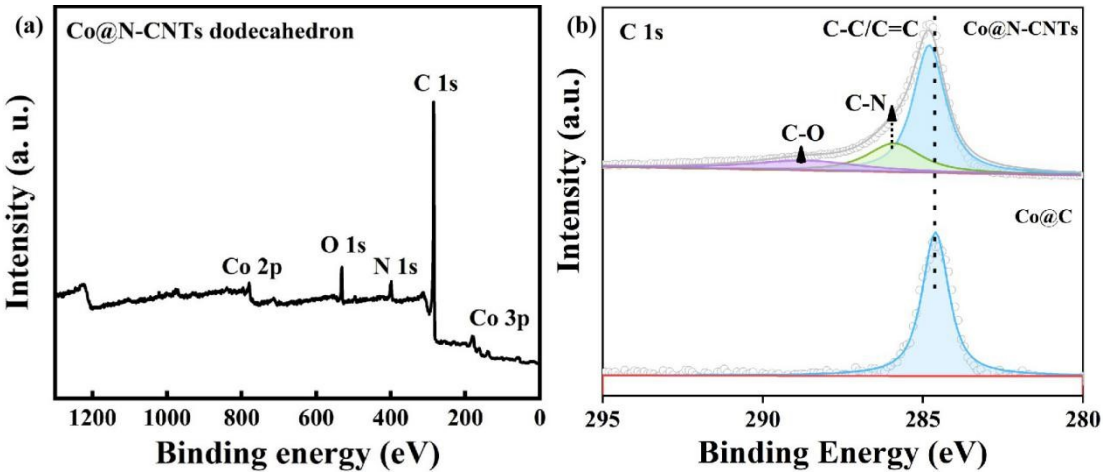

Figure S4. (a) The XPS survey scan of the Co@N-CNTs hollow hybrid dodecahedron framework, (b) The high-resolution XPS spectra of C1s in the Co@N-CNTs and Co@C.

In order to confirm the positive charge sites of carbon atoms nearby N atoms in Co@N-CNTs hollow hybrid dodecahedron framework, we prepared the Co@C composite through the simple hydrothermal reaction followed by high temperature calcination. Then, we compared the C 1s XPS spectra of Co@N-CNTs and Co@C in Figure S4b. It is not difficult to find that the C 1s XPS peak in the Co@N-CNTs is positively shifted (0.2 eV) compared to that in Co@C, indicating that the small electron density transfers from C atoms to N atoms. This observation proves that N-doping brings about the electron delocalization in the doped region. Therefore, the electron density transfer makes C and N atoms in Co/N-CNTs nanozyme have partial positive charge ($C^{\delta+}$) and negative charge ($N^{\delta-}$). The positive charge sites on nearby carbon atoms ($C^{\delta+}$) are benefit to adsorb dissolved oxygen on the surface of Co@N-CNTs catalyst, thus promoting the oxidase-like activity.

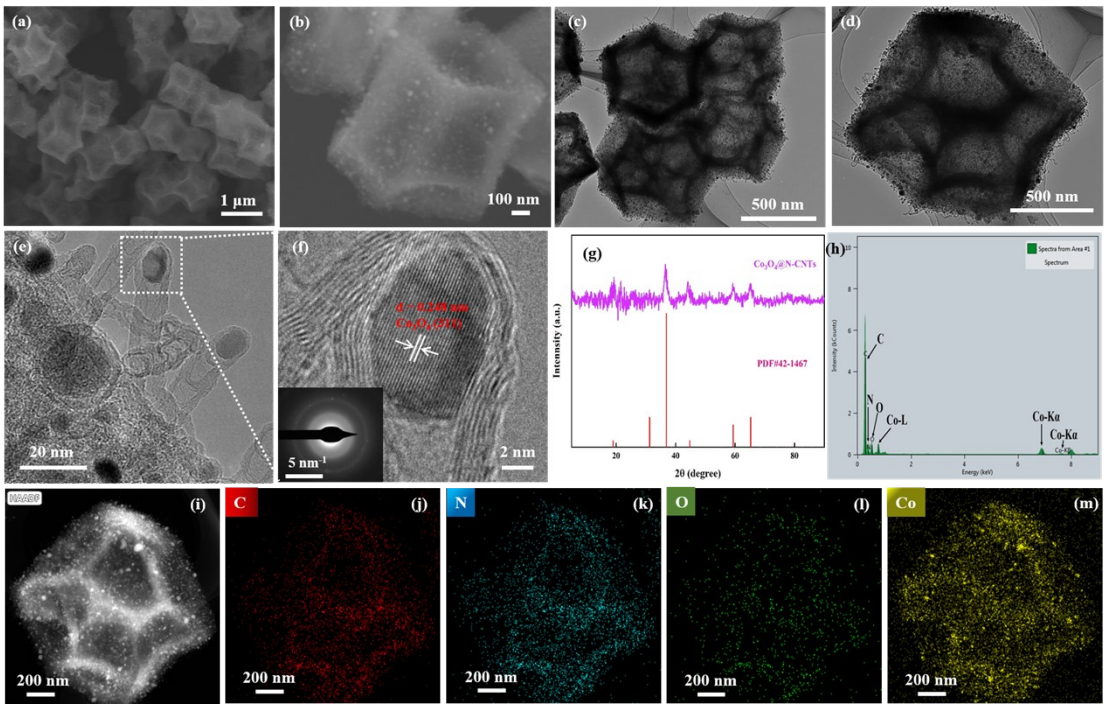

Figure S5. (a-b) the SEM images, (c-e) the stepwise magnified TEM images, (f) HRTEM image (inset is the SAED pattern), (g) XRD pattern, (h) EDX spectrum, (i) HAADF-STEM image and (j-m) EDX elemental mapping images of Co_3O_4@N-CNTs hollow hybrid dodecahedron framework.

In order to emphasize the component and structural advantages of Co@N-CNTs dodecahedron, two contrast materials were also prepared. Firstly, the Co_3O_4@N-CNTs material, which Co_3O_4 nanoparticles are wrapped into N-doped carbon nanotubes inlaying with dodecahedron carbon framework, was synthesized by low-temperature oxidation of Co@N-CNTs in oxygen atmosphere. The SEM (Figure S5a-b) and TEM (Figure S5c-d) images of Co_3O_4@N-CNTs illustrate that the carbon skeleton was not obviously broken even suffering from the oxidation in the air, implying the Co@N-CNTs material owns outstanding structural stability. Besides, as shown in Figure S5e, the grain diameter of Co_3O_4 nanoparticles appears to increase slightly (~ 15 nm) after oxidation, comparing with Co nanoparticles (~ 10 nm) in Co@N-CNTs material. And the wall thickness of N-doped carbon nanotubes seems to be cut down mildly (Figure S5f), owing the the depletion of carbon materials in the air. The HRTEM image in Figure S5f shows the lattice space of 0.248 nm corresponding to the (311) crystal lattice of Co_3O_4. Similar result is also testified by the XRD pattern of Co_3O_4@N-CNTs (Figure S5g), in which four peaks located at 36.5°, 44.1°, 59.2° and 65.1° are attributed to the (311), (400), (511), and (440) facets of Co_3O_4 (PDF no. 42-1467). The EDX and HAADF-STEM elemental mapping in Figure S5h and Figure S5i-m further confirm the presence of C, N, O and Co elements in Co_3O_4@N-CNTs contrast material. The above results prove the successfully synthesis of Co_3O_4@N-CNTs hollow hybrid dodecahedron framework.

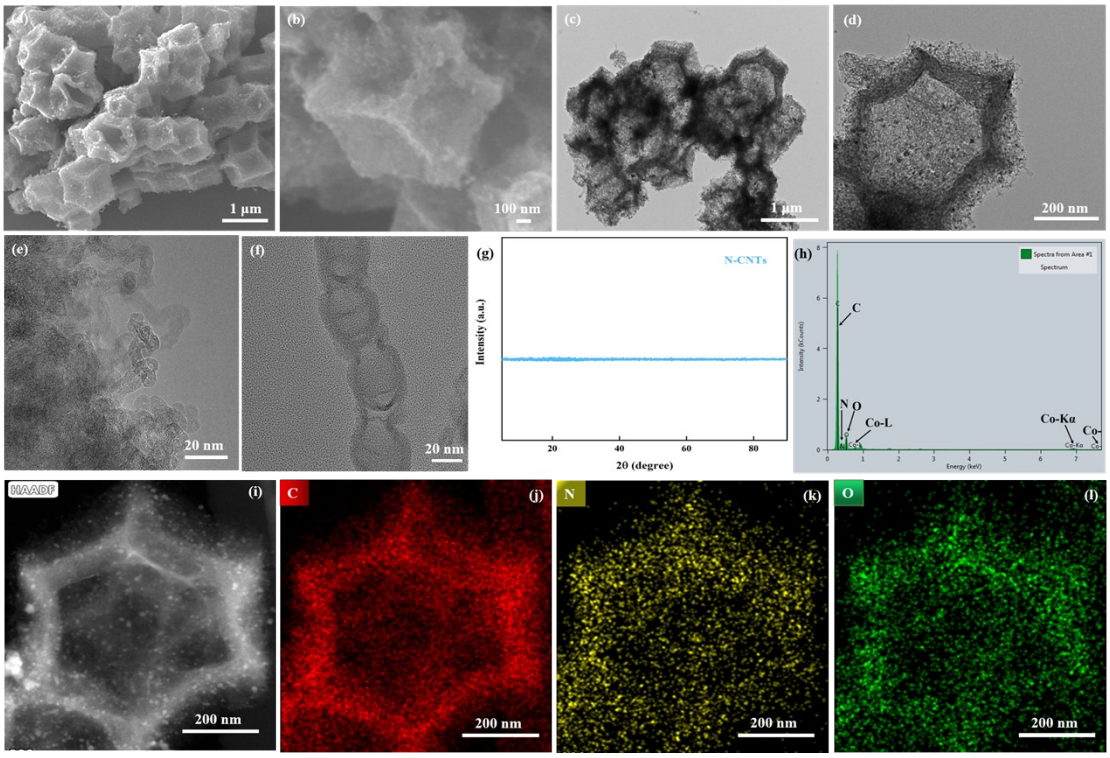

Figure S6. (a-b) the SEM images, (c-f) the stepwise magnified TEM images, (g) XRD pattern, (h) EDX spectrum, (i) HAADF-STEM image and (j-l) EDX elemental mapping images of N-CNTs hollow hybrid dodecahedron framework.

In addition, to elucidate the catalytic effect of Co active nanoparticles, the Co_3O_4@N-CNTs was etched with concentrated hydrochloric acid for 4 hours to obtain N-CNTs dodecahedron without the Co nanoparticles. The SEM and TEM images of N-CNTs in Figure S6a-f display that the inlaid Co nanoparticles almost are dissolved and the residual N-CNTs maintains the dodecahedron morphology of Co_3O_4@N-CNTs without collapse. And the components of N-CNTs dodecahedron are characterized by XRD, EDX and HAADF-STEM elemental mapping in Figure S6g-l. The results demonstrates that the Co nanoparticles are fully etched and N-CNTs hollow hybrid dodecahedron framework is successfully prepared.

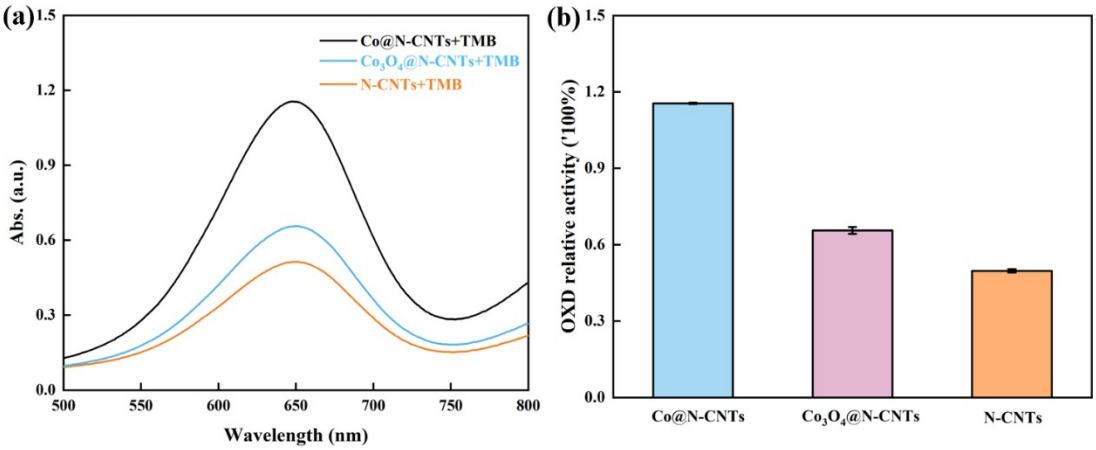

Figure S7. (a) UV-vis absorption spectra of different catalysts (Co@N-CNTs, Co_3O_4@N-CNTs and N-CNTs) with TMB substrate in acetate buffer solution (pH=4.0) recorded at 10 min. (b) The corresponding histogram of oxidase-like relative activity for different catalytic systems.

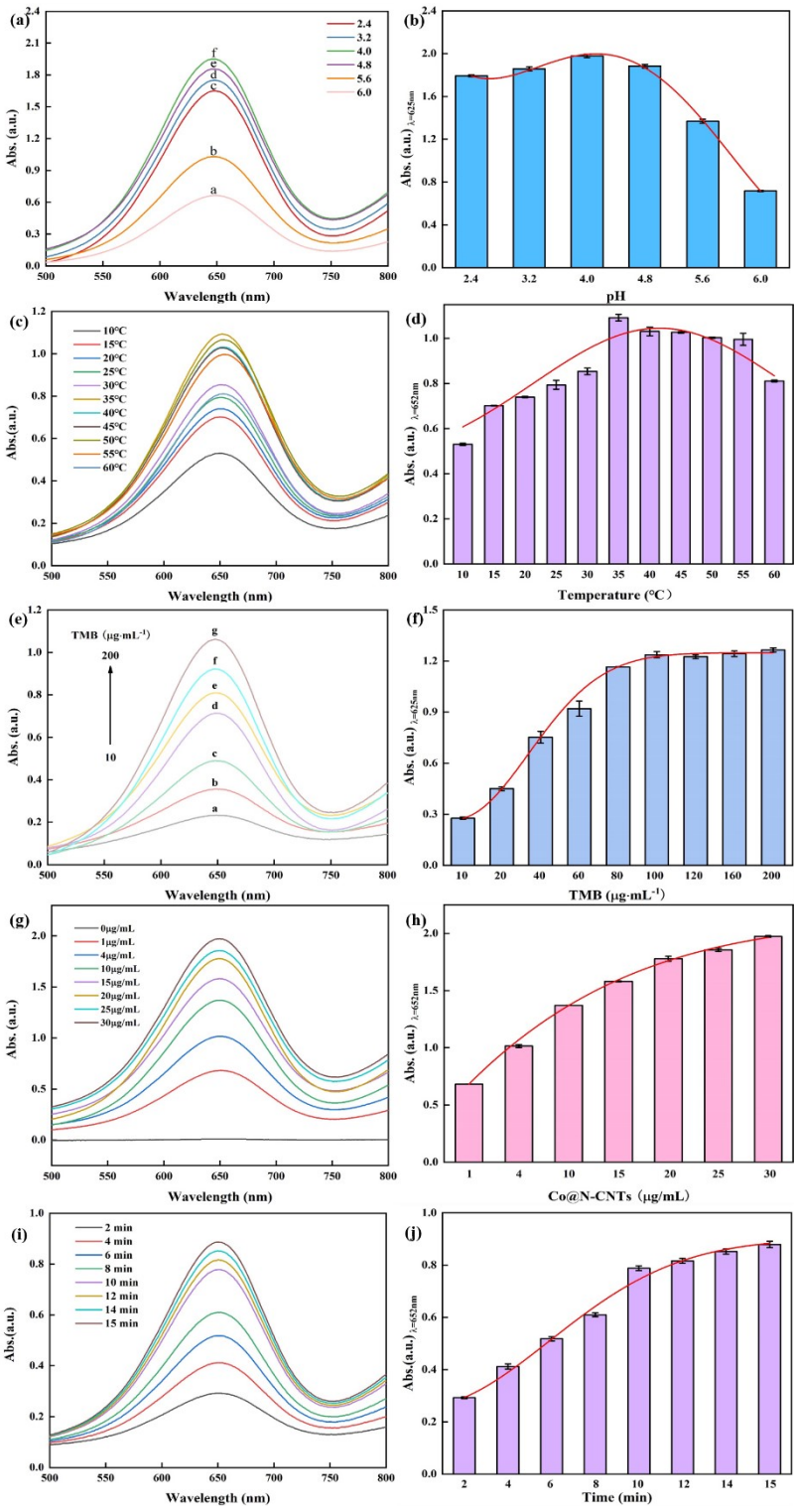

Figure S8. The influences of (a-b) pH, (c-d) temperature, (e-f) TMB concentration, (g-h) catalyst concentration and (i-j) reaction time on the oxidase-like activity of the Co@N-CNTs catalyst. The error bars represent the standard deviation values of three measurements.

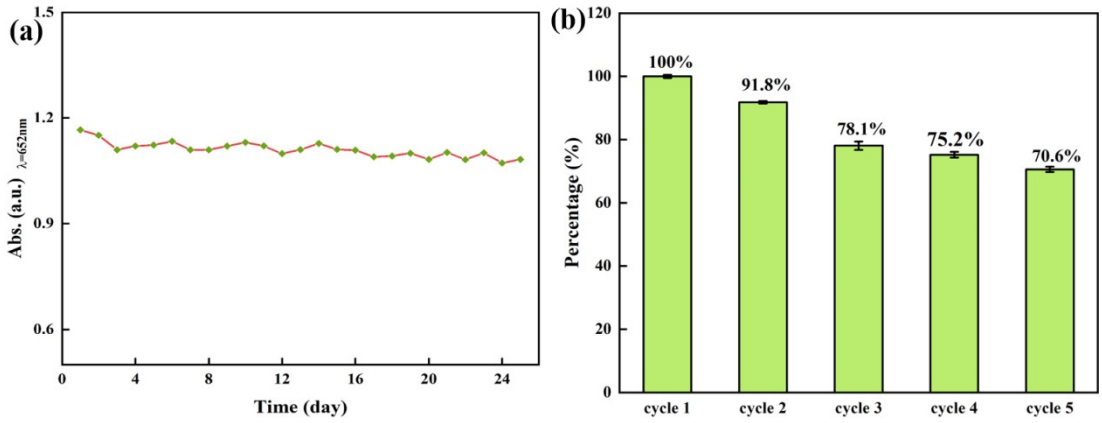

Figure S9. (a) Long-term stability of Co@N-CNTs catalyst for oxidase mimicking. (b)The UV-vis absorption value of relative catalytic activity for five cyclic experiments. (Primary reaction system: 10 μg/mL Co@N-CNTs; 80 μg/mL TMB; HAc-NaAc buffer solution, pH=4).

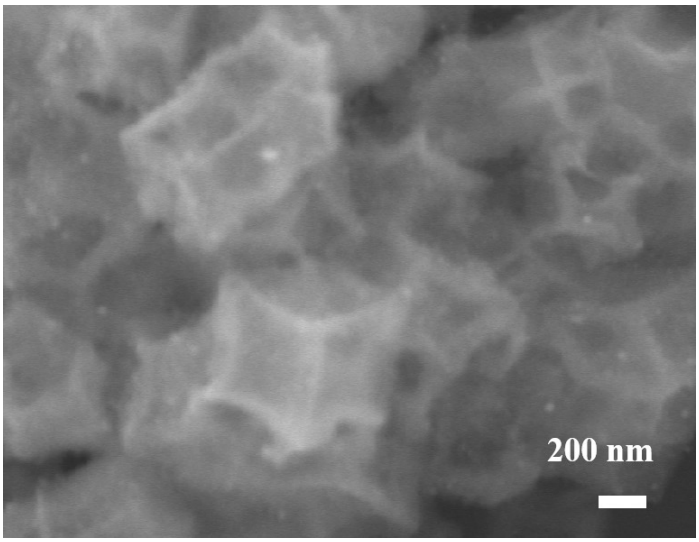

Figure S10. The SEM image of Co@N-CNTs catalyst after the stability test.

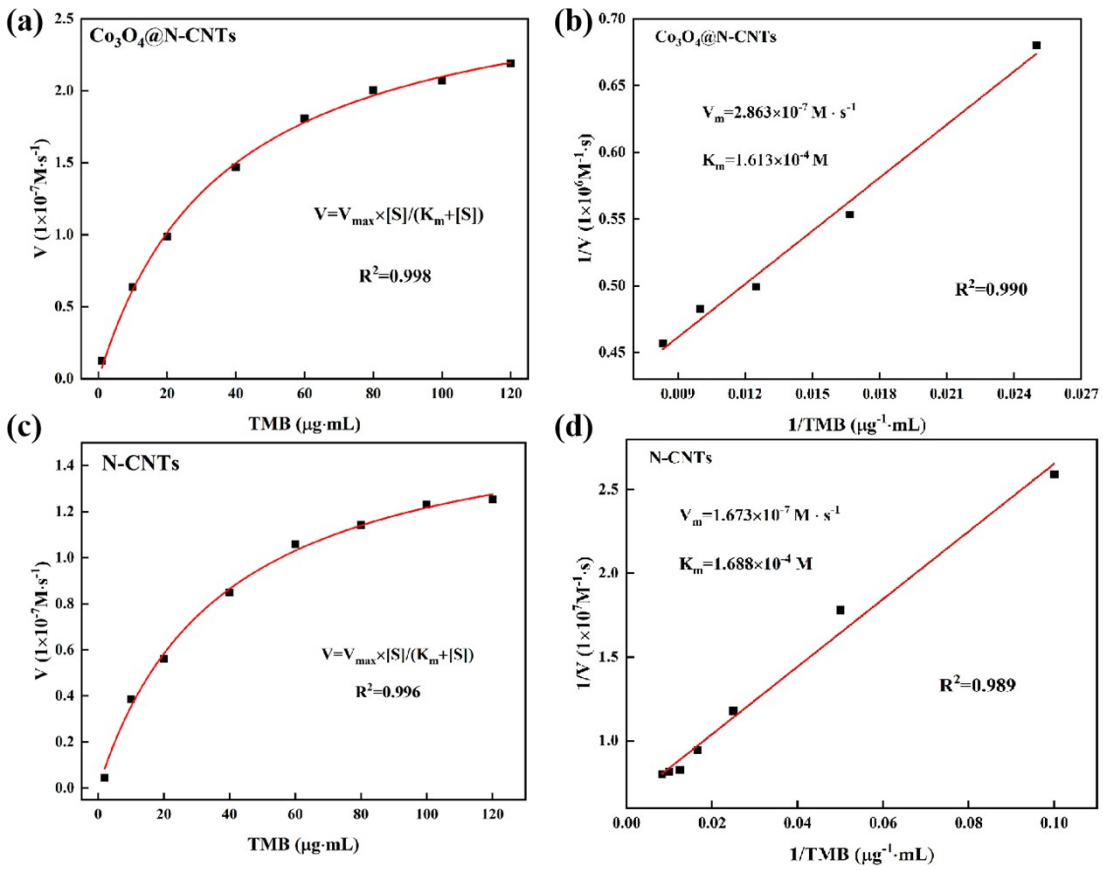

Figure S11. (a) Michaelis-Menten curve and (b) Lineweaver-Burk plots of Co_3O_4@N-CNTs catalyst for oxidase-like activity. (c) Michaelis-Menten curve and (d) Lineweaver-Burk plots of N-CNTs catalyst for oxidase-like activity. The double reciprocal plot of TMB was made from the respective Michaelis-Menten curve.

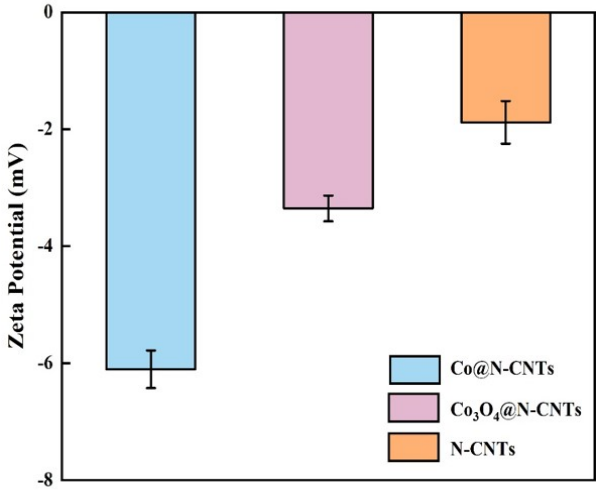

Figure S12. The Zeta potential measurements of Co@N-CNTs, Co_3O_4@N-CNTs, and N-CNTs catalysts. The error bars represent the standard deviation values of three measurements.

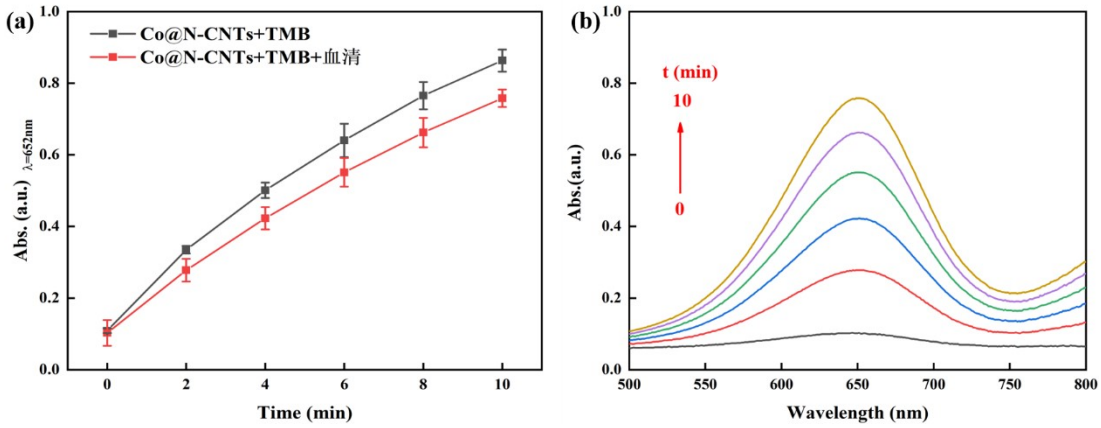

Figure S13. (a) The effect of time on the catalytic activity of Co@N-CNTs on the absence and presence of human serum; (b) The UV-Vis absorption spectrum changes of the time at the range of 500-800 nm. (Reaction system: Co@N-CNTs, 10 μg/mL; TMB, 80 μg/mL; HAc-NaAc buffer solution, pH =4; Serum, 50μL; The reaction time from 0 to 10 minutes).

Table S1. Comparison of the K_m, V_{max} values for Co@N-CNTs nanozyme with those of other mimic oxide enzymes.

System	Signal output	K_m ($\times 10^{-4}$ M)	V_{max} ($\times 10^{-7}$ M·s^{-1})	References
MOF-818 /3,5-DTBC	Colorimetry	8.10	31.7	[1]
$CoSe_2$ hollow micros pheres /TMB	Colorimetry	4.7	1.7	[2]
Co_3O_4 NPs /TMB	Colorimetry	0.5	0.33	[3]
PAA-CeO_2 /TMB	Colorimetry	6	0.31	[4]
CeO_2 NPs /TMB	Colorimetry	4.2	1.004	[5]
Co@N-CNTs/TMB	**Colorimetry**	**1.035**	**3.166**	**This work**

Reference

1. M. Li, J. Chen, W. Wu, Y. Fang and S. Dong, *J. Am. Chem. Soc.*, 2020, **142**, 15569-15574.

2. L. Wang, S. Li, X. Zhang and Y. Huang, *Talanta*, 2020, **216**, 121009-121017.

3. W. Qin, L. Su, C. Yang, Y. Ma, H. Zhang and X. Chen, *J. Agric. Food Chem.*, 2014, **62**, 5827-5834.

4. S.-X. Zhang, S.-F. Xue, J. Deng, M. Zhang, G. Shi and T. Zhou, *Biosens. Bioelectron.*, 2016, **85**, 457-463.

5. H. Cheng, S. Lin, F. Muhammad, Y.-W. Lin and H. Wei, *ACS Sens.*, 2016, **1**, 1336-1343.